Numerical Study of the Propagation Patterns of Lean Hydrogen-Air Flames Under Confinement

Anne Dejoan, Daniel Fernández-Galisteo, Vadim N. Kurdyumov
Dept. of Energy, Centro de Investigaciones Energéticas, Medioambientales y Tecnológicas
Madrid, Spain

1 Introduction

The present work is motivated by the experimental observations on the structure of lean premixed hydrogen-air flames propagating in a Hele-Shaw chamber [1–3]. For large enough distance, h, between the plates of the Hele-Shaw chamber, these experiments show angular sawtooth-shaped flame structures at the large scales and small flame cells at the small scales. However, as the distance h is reduced and becomes close the planar flame thickness, δ_f, the experiments report the existence of isolated flame cells that can propagate steadily in the form of a one-headed or two-headed type and can develop into a fractal-like pattern [2, 3]. This latter phenomenon, observed for very lean hydrogen-air mixtures, is an anomaly to the traditional quenching limit given by a Peclet number, $Pe = h/\delta_f$, of order 40 [4]. Such combustion regime is of particular relevance for safety issues in the storage and use of hydrogen.

Propagation of lean hydrogen-air flames have been studied in a two-dimensional (2D) domain employing detailed chemistry and transport [5, 6]. These works report the angular sawtooth shapes and the cellular structures in agreement with [1] for large h. In cases of small h, 2D simulations can not capture the effects of confinement (losses of momentum and heat) inherent to the Hele-Shaw chamber when the plates are very close. In this work, we propose to analyze these confinement effects by making use of numerical simulations within the quasi-2D approximation [7–9] and employing the one-step reduced kinetics [10] to describe the chemistry of the hydrogen-air combustion. The momentum loss effects are analyzed by comparing the overall propagation and structure of the flame obtained from 2D and quasi-2D simulation results. The modification of the flame propagation and structure in the presence of heat loss is given for different amounts of heat losses representative of very small gap distances.

2 Governing Equations

In the limit of very small distance between the plates of the Hele-Shaw burner ($h/\delta_f \rightarrow 0$), the 3D reactive Navier-Stokes equations written in the low-Mach number approximation can be reduced to the

Correspondence to: anne.dejoan@ciemat.es

following 2D set of equations

$$\frac{\partial \rho}{\partial t} + \nabla\cdot(\rho \mathbf{v}) = 0, \tag{1}$$

$$\mathbf{v} = -\frac{h^2}{12\mu}\nabla p, \tag{2}$$

$$\frac{\partial}{\partial t}(\rho Y_k) + \nabla\cdot(\rho \mathbf{v} Y_k) = \frac{1}{Le_k}\nabla\cdot\left(\frac{\lambda}{c_p}\nabla Y_k\right) + \dot{\omega}_k W_k, \tag{3}$$

$$\frac{\partial}{\partial t}(\rho T) + \nabla\cdot(\rho \mathbf{v} T) = \nabla\cdot\left(\frac{\lambda}{c_p}\nabla T\right) + \frac{\lambda}{c_p^2}\nabla c_p\cdot\nabla T - \frac{1}{c_p}\sum_{k=1}^{N} h_k\,\dot{\omega}_k W_k - \frac{b}{c_p}\,(T - T_{\mathrm{w}}), \tag{4}$$

where $\mathbf{v}$, ρ, p, T stand for the velocity, density, pressure and temperature, respectively; Y_k, h_k, $\dot{\omega}_k$ and W_k denote the mass fraction, enthalpy, reaction rate, and molecular weight of the species k; μ is the dynamic viscosity; Le_k the Lewis number of species k; λ and c_p the thermal conductivity and the heat capacity of the gas mixture; T_{w} the temperature of the outer walls of the plates and is fixed to the ambient temperature, $T_{\mathrm{w}} = 298$ K. The mixture follows the equation of state of ideal gas with constant thermodinamic pressure, P.

Within this formulation, referred to as the quasi-2D approximation, the flow properties are averaged accross the gap distance h and the momentum equation is reduced to the linear relation (2) for the velocity field, similar to Darcy's law. The heat-loss parameter, $b = 2\lambda_{\mathrm{w}}/hh_{\mathrm{w}}$ (with λ_{w} and h_{w} the thermal conductivity and the thickness of the solid wall material, respectively), in Eq. 4 accounts for the conductive losses averaged between the plates. For further details on the derivation of the quasi-2D formulation the reader is referred to [7, 8].

The chemistry is described by the one-step reduced kinetics for lean hydrogen-air deflagrations developed in [10]. This chemistry employes only $N = 3$ species (H_2, O_2, and H_2O) instead of the 8 species (H_2, O_2, H_2O, H, O, OH, HO_2, and H_2O_2) involved in the detailed chemistry. Compared to the fully detailed chemistry, the one-step kinetics has the advantage to include the main steps of chemical reactions and tackle the relevant physics of lean hydrogen combustion at a low cost. In all the simulations presented here the equivalence ratio is $\phi = 0.4$, the fresh mixture temperature is set to $T_u = 298$ K and the constant mixture thermodynamic pressure takes the value $P = 1$ atm. The species diffusivities are imposed by setting spatially homogeneous Lewis numbers, with $Le_{\mathrm{H_2}} = 0.3$, $Le_{\mathrm{O_2}} = 1.11$, and $Le_{\mathrm{H_2O}} = 0.83$. The thermal conductivity of the gas mixture is computed with the approximation $\lambda/c_p = 2.58 \times 10^{-4}(T/T_u)^{0.7}$ g/(cm·s), with c_p evaluated by NASA polynomials. The Soret effects are not included. For the considered equivalence ratio, fresh mixture temperature, diffusion coefficients, and transport model, the planar flame velocity and the flame thickness computed with the one-step kinetics take the values $S_L = 32.8$ cm/s and $\delta_f = 0.06$ cm (with δ_f defined on the maximum temperature gradient).

In addition to the quasi-2D problem given by Eqs. (1)-(4), numerical simulations are also performed with the full set of the Navier-Stokes, temperature and species equations written in the 2D frame (making use of the same one-step kinetics and flame parameters than those described above). These additional simulations solve the momentum equation instead of (2). These (unconfined) 2D simulations allow to identify momentum-loss effects by direct comparisons with the results obtained from the quasi-2D simulations. Moreover, they provide possible comparisons with the 2D results given in [6] where detailed chemistry was used (see Sec. 3.1).

2 Numerical Treatment

The numerical simulation code used for the integration of the governing equations is the Open source Field Operation And Manipulation (Open-FOAM) toolbox [11]. The equations are discretized on a collocated grid arrangement making use of the finite volume method. The PIMPLE algorithm is applied for the pressure-velocity coupling to ensure mass conservation. Temporal discretization is performed through a first-order Euler scheme while a second-order scheme is used for spatial discretization.

The computational domain is large enough to contain the main flame scales, with the dimensions $L_x \times L_y$ in the longitudinal and transversal directions, respectively. In the 2D and quasi-2D adiabatic simulations (see Sec. 3.1) $L_x = L_y = 200\delta_f$. A uniform cartesian grid is used with the grid resolution $\Delta_x = \Delta_y = 0.1\delta_f$. When heat loss is accounted for in the quasi-2D simulations (see Sec. 3.2), the transversal domain size is reduced to $L_y = 50\delta_f$ and the mesh resolution is refined such that $\Delta_x = \Delta_y = 0.05\delta_f$. The time step is small enough to maintain numerical stability and takes the value $\Delta t = 10^{-3}\delta_f/S_L$.

Boundary conditions are $p = 0$ atm and $\partial T/\partial x = \partial Y_k/\partial x = 0$ at $x = 0$ and $\mathbf{v}_\mathrm{x} = \partial T/\partial x = \partial Y_k/\partial x = 0$ at $x = 200\delta_f$, so the flame front propagates towards increasing x. Periodic boundary conditions are used in the transversal direction y.

In the adiabatic simulations, the computations are initiated with the planar unstretched premixed flame solution to which a sinusoidal pertubation with small amplitude is added. Then, the time evolution of the front flame is followed up to reach a well-established state. The total time of the simulations is around $t = 170\delta_f/S_L$. To initiate the quasi-2D simulations with heat loss, a long-term solution of the flow field from the adiabatic quasi-2D case has been used.

3 Results

3.1 Momentum-Loss Effects

The effect of momentum loss is shown in Fig. 1 (left) by comparing the time evolution of the consumption speed, $S_c = (\rho_u Y_{\mathrm{H}_{2,\mathrm{u}}} L_y)^{-1} \int_0^{L_x}\int_0^{L_y} \dot{\omega}_{\mathrm{H}_2}\,\mathrm{d}x\,\mathrm{d}y$ (with $\dot{\omega}_{\mathrm{H}_2}$ the hydrogen consumption rate), as obtained for the 2D and the quasi-2D formulation. For the quasi-2D formulation, $b = 0$ cal/(cm^3·s·K) is set in the temperature equation (4) to represent adiabatic walls. Figure 1 (left) exhibits well-established time evolutions for both cases and shows higher values of S_c in the presence of momentum loss compared to the 2D case, for which this effect is absent. Instantaneous 2D and quasi-2D flame fronts are illustrated in Fig. 2. Under momentum loss the corrugated flame front tends to form more elongated cells in a finger-like structure, thus increasing the total flame surface area and the consumption speed. Also, the maximum temperature located around the head of the cells is higher in the quasi-2D case (1760 K) than for the 2D case (1610 K). The increase of temperature leads to larger $\dot{\omega}_{\mathrm{H}_2}$ and thus larger consumption speed as well. Note that, because flame curvature promotes differential diffusion, both temperatures are above the adiabatic one (1438 K).

It is worth to mention that the flame structure drawn in Fig. 2 (left) is in satisfactory agreement with that reported in [6], where authors present 2D simulations of lean hydrogen-air flames with identical flame parameters as considered here but employing detailed chemistry. In particular, for the computational domain size marked in Fig. 2 with rectangular white boxes, the present 2D case shows characteristic sizes of the large and the small flame scales comparable to those given for the same domain in [6]. Moreover, we find a normalized time-averaged consumption speed $\overline{S}_c/S_L \sim 4.4$, while [6] reports a value of 4. By including the Soret effects this difference should be reduced.

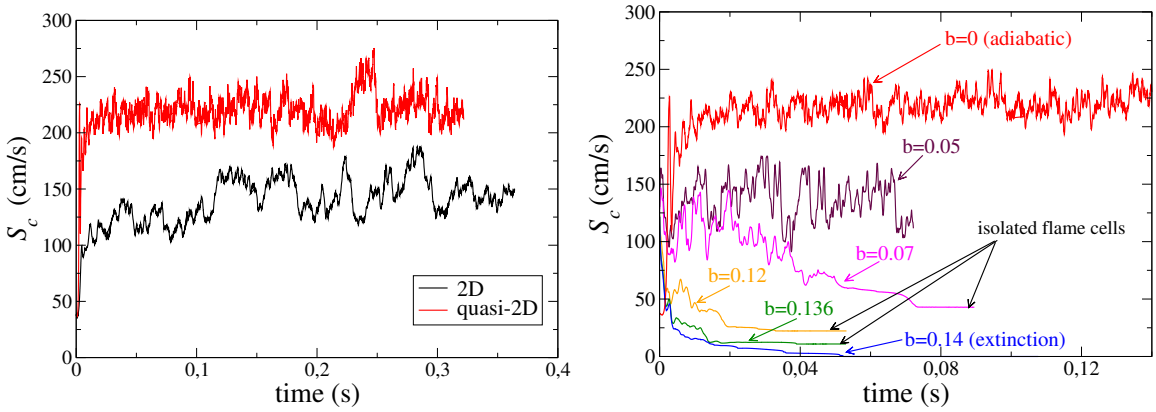

Figure 1: Time evolution of the consumption speed S_c. Left: 2D and quasi-2D ($b = 0$) simulations. Right: quasi-2D simulations for different values of b.

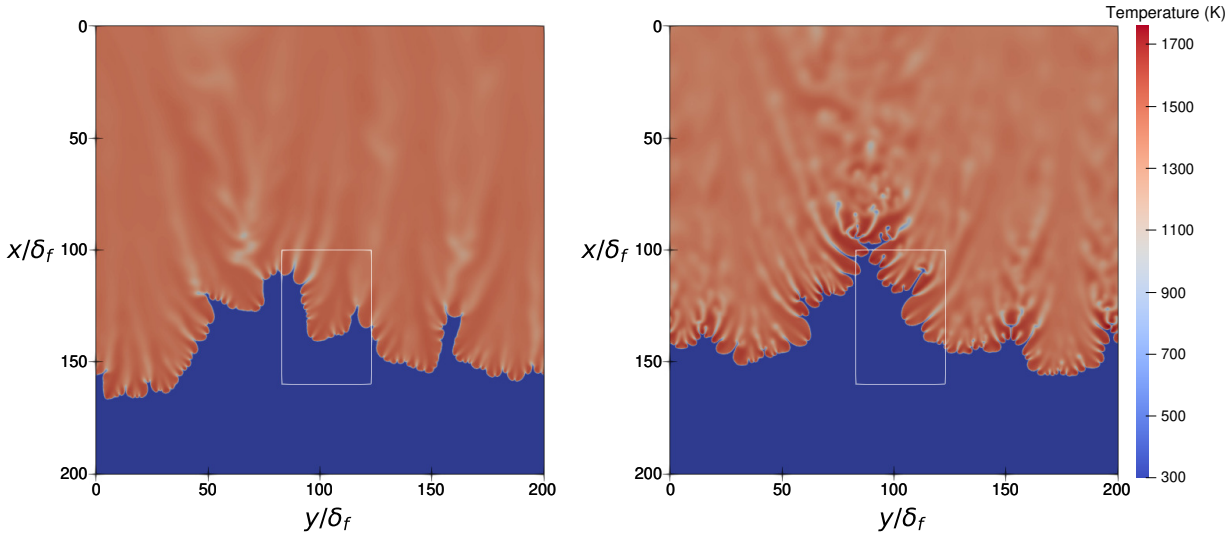

Figure 2: Visualization of the temperature field at time $t = 0.3$ s ($\sim 165\delta_f/S_L$). Left: 2D simulation. Right: quasi-2D simulation. The dimensions of computational domain are rescaled with the flame thickness δ_f. The white box ($60\delta_f \times 40\delta_f$) is drawn to highlight the characteristic flame scales as done in [6].

3.2 Heat-Loss Effects

In the following, the heat-loss effect is analyzed in the quasi-2D formulation. Not shown here, in the presence of heat loss the flame front tends to flatten and the large scales present in the computational domain of Fig. 2 (right) desappear while the small-scale flame cells remain. For this reason, the width of the domain size can be reduced in this section to $L_y = 50\delta_f$ (large enough to contain the main flame scales). The grid resolution has been refined to $\Delta_x = \Delta_y = 0.05\delta_f$ to correctly tackle the appearence of isolated flame cells as the heat loss increases.

Figure 1 (right) shows that, as expected, increasing b reduces the consumption speed S_c. For $b \geq 0.14$ cal/(cm^3·s·K) flame extinction occurs. In Fig. 3 the water mass fraction, $Y_{\mathrm{H_2O}}$, has been selected as a marker for tracking the front evolution. For $b \geq 0.7$ cal/(cm^3·s·K) isolated two-headed flame cells are observed to propagate throughout the chamber. As shown in Fig. 1 (right), the propagation speed of these fingers reaches a steady state, at least for the observed times. The steady character of this two-headed cell has been recently reported in [9], using a simple Arrhenius chemistry model. The characteristic size of the cells (indicated by white arrows in Fig. 3) disminishes as b increases, varying between $6.7\delta_f$ and $4.2\delta_f$. This size is close to the value of $6\delta_f$ reported by [6] for the adiabatic and unconfined 2D case. Also observed, is the larger separation between the two heads of the flame cell with the increase of b. The pattern obtained here for $b = 0.12$ and 0.136 cal/(cm^3·s·K) is very similar to that observed in the experiments [2, 3], as well as the cell size (around 2 or 3 mm). It is worth noting that the displacement velocity, S_d, of the isolated flame patterns (much appropriate to consider than S_c in these cases) can be greater than the laminar flame S_L. As for example, in the case $b = 0.136$ cal/(cm^3 s K) the two-headed cell propagates at $S_d \sim 2S_L$. The characteristics of the flame patterns corroborate quite well with the experiments, however the lateral motion found in the present simulations was not observed in [2]. Similar lateral motions were also reported in previous numerical studies in unconfined 2D geometries, as for example in [6]. This requires further examination to be explained.

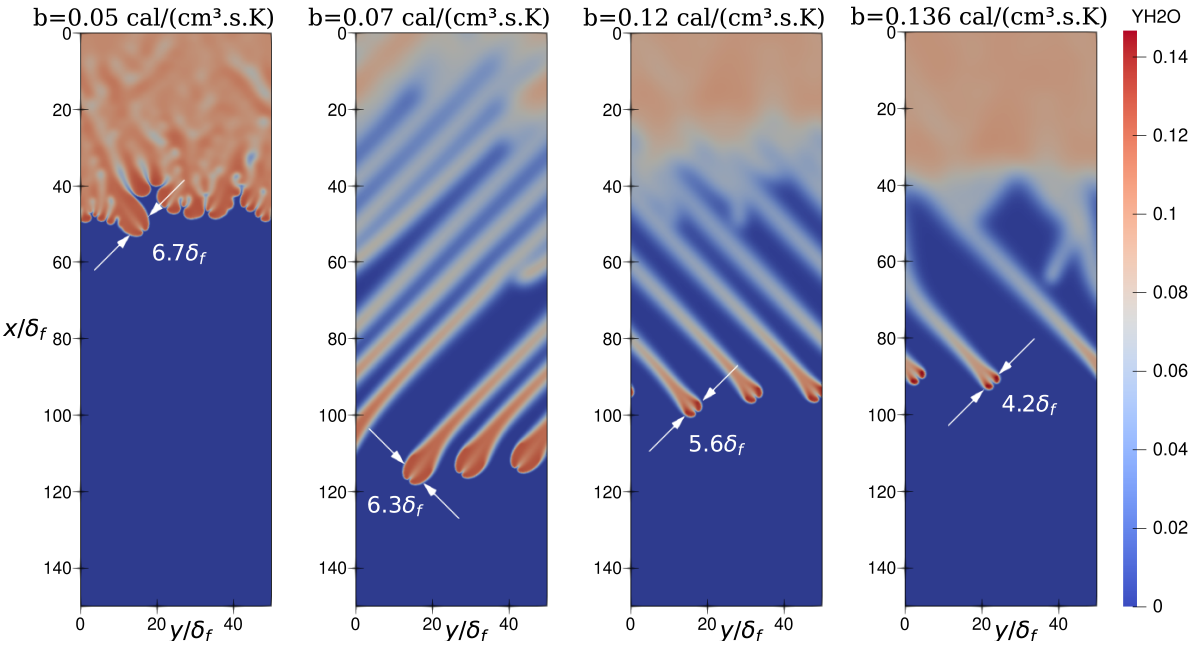

Figure 3: Visualization of the water mass fraction, $Y_{\mathrm{H_2O}}$, field given for different values of the heat-loss parameter b. The dimensions of computational domain are rescaled with the flame thickness δ_f. White arrows indicate flame finger size in non-dimensional units.

4 Conclusions

The present study reports numerical simulations of lean premixed hydrogen-air flame propagating in a Hele-Shaw chamber. The effects of momentum and heat, inherent to this confined geometry, are analyzed by employing a quasi-2D formulation based on Darcy's law. This formulation allows us to reduce the original 3D dimensionality of the problem to 2D with the flow properties averaged between the plates of the chamber. Hydrogen chemistry is described by a one-step reduced mechanism. This mechanism (in agreement with a more detailed chemistry) reproduces the main flame characteristics observed in the experiments. The momentum-loss effects are examined in the adiabatic case by comparing results obtained from a unconfined 2D formulation and from the quasi-2D formulation. The momentum loss is shown to further corrugate the flame front (compared with the unconfined 2D case) leading to more finger-like shapes, increasing, in turn, the consumption speed. In presence of heat loss, finger patterns develop and isolated flame cells form. Their characteristic size decreases with the increase of heat loss, and it is found to be four to six times the laminar flame thickness with a displacement velocity higher than the laminar flame velocity.

References

[1] Shen S, Wongwiwat J, Gross J, Ma X, Ronney P.D. (2016). Flame propagation in narrow channels at varying Lewis numbers. WSSCI Spring Meeting 2016: 139LF-0020.

[2] Veiga-López F, Kuznetsov M, Martínez-Ruiz D, Fernández-Tarrazo E, Grune J, Sánchez-Sanz M. (2020). Unexpected propagation of ultra-lean hydrogen flames in narrow gaps. Phys. Rev. Lett. 124: 174501.

[3] Yañez J, Kuznetsov M, Veiga-López F. (2021). Characterization of unconventional hydrogen flame propagation in narrow gaps. Phys. Rev. E 103: 033101.

[4] Jarosinski J. (1983). Flame quenching by a cold wall. Combust. Flame 50: 167.

[5] Altantzis C, Frouzakis CE, Tomboulides AG, Kerkemeier SG, Boulouchos K. (2011). Detailed numerical simulations of intrinsically unstable two-dimensional planar lean premixed hydrogen/air flames. Proc. Combust. Inst 33: 1261.

[6] L. Berger and K. Kleinheinz and A. Attili and H. Pitsch. (2019). Characteristics patterns of thermodiffusively unstable premixed kean hydrogen flames. Proc. Combust. Inst. 37: 1879.

[7] Fernández-Galisteo D, Kurdyumov VN, Ronney PD. (2018). Analysis of premixed Flame propagation between two closely-spaced parallel plates. Combust. Flame 190: 133.

[8] Martínez-Ruiz D, Veiga-López F, Fernández-Galisteo D, Kurdyumov VN, Sánchez-Sanz M. (2019). The role of conductive heat losses on the formation of isolated flame cells in Hele-Shaw chambers. Combust. Flame 209: 187.

[9] Domínguez-González A, Martínez-Ruiz D, Sánchez-Sanz M. (2022). Stable circular and double-cell lean hydrogen-air premixed flames in quasi two-dimensional channels. Proc. Combust. Inst. In press.

[10] Fernández-Galisteo D, Sánchez AL, Liñán A, Williams FA. (2009). One-step reduced kinetics for lean hydrogen-air deflagration. Combust. Flame 156: 985.

[11] https://www.openfoam.com/